

Anharmonic phonons and high-temperature superconductivity

Vincent H. Crespi and Marvin L. Cohen

*Department of Physics, University of California at Berkeley,
and Materials Sciences Division, Lawrence Berkeley Laboratory, Berkeley, California 94720*

(Received 6 December 1991; revised manuscript received 29 October 1992)

We examine a simple model of anharmonic phonons with application to the superconducting isotope effect. Linear and quadratic electron-phonon coupling are considered for various model potentials. The results of the model calculations are compared with the high-temperature superconductors $\text{La}_{2-x}\text{Sr}_x\text{CuO}_4$, $\text{Y}_{1-x}\text{Pr}_x\text{Ba}_2\text{Cu}_3\text{O}_{7-\delta}$, and $\text{YBa}_2\text{Cu}_{3-x}\text{M}_x\text{O}_{7-\delta}$ with $M=\text{Zn, Ni, or Fe}$.

I. INTRODUCTION

Numerous experimental and theoretical results bear on the importance of the electron-phonon interaction in the high-temperature superconductors. Theoretical calculations indicate that the roughly 30 K transition temperature of the noncuprate superconductor $\text{Ba}_{1-x}\text{K}_x\text{BiO}_3$ can be explained with standard electron-phonon coupling.¹ Tunneling measurements on $\text{Ba}_{1-x}\text{K}_x\text{BiO}_3$ and $\text{Nd}_{2-x}\text{Ce}_x\text{CuO}_4$ support a phonon-mediated mechanism.² Tunneling results for Y-Ba-Cu-O can also be interpreted as suggesting strong electron-phonon coupling.³ Indications of phonon softening at the superconducting transition suggest significant coupling between the electrons and certain phonon modes.^{4,5} Several anomalous properties of the high-temperature superconductors can be explained within an electron-phonon framework. For example, the lack of a coherence peak in the nuclear spin relaxation time can be ascribed to strong coupling effects.⁶ Discounting possible effects due to thermal expansion,⁷ the lack of saturation in high-temperature resistivity data appears to be inconsistent with a system having strong electron-phonon coupling.⁸ However, explanations exist incorporating anisotropic electron-phonon coupling⁹ or variations in the Fermi velocity across the Fermi surface.¹⁰

The small isotope effect argues against a phonon mechanism, but anharmonic effects could circumvent this objection. The large variations in the isotope effect exponent with doping in $\text{La}_{2-x}\text{Sr}_x\text{CuO}_4$ can be explained by doping-dependent anharmonic potentials.¹¹ It is difficult to explain the large isotope effect at certain Sr concentrations if phonons do not contribute to

the pairing. Other varieties of doping, such as Pr for Y (Ref. 12) or Fe for Cu,¹³ also produce high- T_c materials with isotope effect exponents on the order of one-half. Frozen-phonon calculations yield strongly anharmonic potentials for certain phonon modes in both $\text{La}_{2-x}\text{Sr}_x\text{CuO}_4$ and $\text{YBa}_2\text{Cu}_3\text{O}_7$.¹⁴ Measurements of pair distribution functions from neutron scattering imply local structural distortions of the Cu-O planes in $\text{La}_{2-x}\text{Sr}_x\text{CuO}_4$, $\text{Tl}_2\text{Ba}_2\text{CaCu}_2\text{O}_8$, and $\text{Nd}_{2-x}\text{Ce}_x\text{CuO}_4$ corresponding to buckling motions of oxygen atoms perpendicular to the Cu-O bond,¹⁵ with indications that the distortions are dynamic.¹⁶ Finally, ion channeling¹⁷ and x-ray absorption¹⁸ experiments suggest strongly anharmonic phonons.

II. THEORY

We shall examine a simplified model of anharmonic phonons in superconductivity. The electron-phonon coupling at zero temperature can be generalized to the anharmonic case by including matrix elements over all of the phonon excited states.¹⁹ Since certain anharmonic modes involve large ionic excursions, the quadratic term in the expansion of the electron-ion potential will be included. The zero temperature form for the electron-phonon coupling should be valid for transition temperatures sufficiently below the relevant phonon frequency, as will be the case for moderately strong coupling. Above $\lambda \approx 2$, we expect a finite temperature treatment to be necessary. We begin with an expression for the electron-phonon coupling constant λ involving a sum over all phonon excited states labeled by the index n ,

$$\lambda = N(0) \sum_{kk'} \sum_{n=1}^{\infty} \frac{\langle n | \langle k' | [(\nabla V \cdot \delta \mathbf{R})_{R_0} + \nabla_i \nabla_j V \delta \mathbf{R}_i \delta \mathbf{R}_j] | k \rangle | 0 \rangle|^2}{E_n - E_0}, \quad (1)$$

where $N(0)$ is the density of states at the Fermi level, $V(r)$ is the electron-ion potential, and $\delta \mathbf{R}$ is the ionic displacement from the equilibrium position R_0 . The sum over k and k' is performed over the Fermi surface. Phonon dispersion has been neglected. Assuming, for ex-

ample, a phonon mode polarized in the x direction, we obtain

$$\lambda = \sum_{n=1}^{\infty} \left[\langle I^2 \rangle \frac{|\langle n | x | 0 \rangle|^2}{E_n - E_0} + \langle J^2 \rangle \frac{|\langle n | x^2 | 0 \rangle|^2}{E_n - E_0} \right], \quad (2)$$

where the prefactors $\langle I^2 \rangle$ and $\langle J^2 \rangle$ contain the electronic contributions and the summation involves matrix elements between phonon states. The electronic degrees of freedom have been factored out, following the treatment of McMillan.²⁰

We have included only one diagram of second order in the expression for λ (or equivalently, the expression for the electronic self-energy). In particular, we have included contributions of the form shown in Fig. 1(a), but ignored diagrams of the form shown in Fig. 1(b). Diagram (a) has one intermediate electronic state, whereas diagram (b) has two. The dominant contributions to the coupling arise from regions of integration where the intermediate electronic states are near the Fermi surface. In diagram (a), this condition puts one constraint on $\vec{Q}_1 + \vec{Q}_2$ (namely, $\vec{Q}_1 + \vec{Q}_2$ must bridge the Fermi surface). In diagram (b), this condition puts constraints on \vec{Q}_1 and \vec{Q}_2 individually. Diagram (a) produces contributions to the coupling over a significantly larger portion of the phonon phase space. For this reason, contributions of the form shown in Fig. 1(a) are assumed to dominate the second-order electron-phonon coupling.

The various energy level differences ($E_n - E_0$) and their contributions to λ are used to create an expression for $\alpha^2 F$,

$$\alpha^2 F(\omega) = \sum_{n=1}^{\infty} \lambda_n \omega_n \delta(\omega - \omega_n), \quad (3)$$

where

$$\lambda_n = \left[\langle I^2 \rangle \frac{|\langle n|x|0 \rangle|^2}{E_n - E_0} + \langle J^2 \rangle \frac{|\langle n|x^2|0 \rangle|^2}{E_n - E_0} \right] \quad (4)$$

and

$$\omega_n = E_n - E_0. \quad (5)$$

For a one-dimensional interionic potential, the numerical solution of the Schrödinger equation is straightforward. The two-dimensional and three-dimensional Schrödinger equations are solved by expansion with a basis of eigenfunctions of the harmonic oscillator. For each energy level, we calculate the mass dependence of ω_n and λ_n and solve the three-dimensional isotropic Eliashberg equations numerically to obtain T_c and α . Since the electronic prefactor in the expression for λ is unknown, we cannot calculate the absolute value of $\frac{d\lambda}{dM}$. Instead, we calculate $\frac{M}{\lambda} \frac{d\lambda}{dM}$, a measure of the relative sensitivity of λ to variations in the oscillator mass.

The model does not include phonon dispersion or Debye-Waller factors in the interionic potential. In ad-

dition, the Eliashberg equations are assumed to be applicable, although there is no rigorous justification for extending the scope of the harmonic T_c equations. A self-consistent treatment of phonon anharmonicity yields expressions which are formally identical to the Eliashberg equations with a fully anharmonic expression replacing the spectral density of the one-phonon Green function.²¹ Unfortunately, the equations are computationally intractable. We propose a simple form for this spectral density, within an Einstein model in which phonon-phonon interactions can be neglected. This treatment, although decidedly less rigorous, has the virtue of computational simplicity. Additional discussion of the approximations inherent in the model is given in previous publications.¹¹⁻²²

III. ANALYTIC RESULTS

Analytic results can be obtained for certain interionic potentials. The Kresin-Barbee-Cohen T_c equation,^{23,24}

$$T_c = 0.26 \frac{\sqrt{\langle \omega^2 \rangle}}{\sqrt{e^{\frac{1}{\alpha}} - 1}}, \quad (6)$$

yields an isotope effect exponent

$$\alpha = \frac{1}{2} - \lambda_M \left[\frac{e^{\frac{1}{\alpha}}}{(e^{\frac{1}{\alpha}} - 1)\lambda} - \frac{1}{2} \right], \quad (7)$$

where

$$\lambda_M = \frac{M}{\lambda} \frac{d\lambda}{dM}. \quad (8)$$

The term in square brackets is always positive, so that a positive (negative) λ_M produces $\alpha < 0.5$ ($\alpha > 0.5$). This equation assumes that $\langle \omega^2 \rangle$ is an accurate measure of the average phonon frequency, since the expression for $\langle \omega^2 \rangle$ provides a sum rule which is used to eliminate the mass dependence of ω from the equation for α .²² This sum rule result is strictly valid only for linear coupling with certain exceptions as noted below. The Eliashberg results for α and T_c for various potentials can be approximated reasonably well with Eqs. (6) and (7).

We first examine the limit of a strong double well, which is approximated as a pair of negative δ -function potentials at $\pm a$. For simplicity, we initially include only linear electron-phonon coupling. A potential of the form

$$V(x) = -\frac{V_0 \hbar^2}{2Ma} [\delta(x+a) + \delta(x-a)] \quad (9)$$

yields equations for the ground state and first excited state in which the energy level and oscillator mass always appear as a product, implying that $\omega_M = -1$ (where $\omega_M \equiv \frac{M}{\omega} \frac{d\omega}{dM}$). The sum rule relation then yields $\lambda_M = 1$ so that the isotope effect exponent is decreased below 0.5. The double δ -function potential has a single length scale, the separation between the wells, which is independent of the ionic mass, so that both the dipole and quadrupole matrix elements in Eq. (4) are mass independent. For this reason, the inclusion of quadratic coupling will not change the mass dependence of λ or ω .

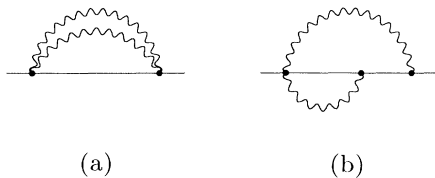


FIG. 1. Second-order contributions to the electron-phonon coupling.

Potentials of the form $V(x) = x^{2n}$ can also be examined analytically in the case of quadratic coupling. Simple scaling arguments yield the mass dependence of the phonon frequencies. For linear coupling, a sum rule relation provided the mass dependence of λ . For quadratic coupling, we approximate the matrix element of x^2 with the square of the classical turning point. Numerical solutions of Schrödinger's equation support this approximation. The strong coupling limit for α can be obtained from the asymptotic strong coupling T_c equation²⁵

$$T_c = 0.18\sqrt{\lambda\langle\omega^2\rangle}. \quad (10)$$

For second-order electron-phonon coupling, the harmonic and pure quartic potentials limit to $\alpha = \frac{3}{4}$ and $\alpha = \frac{2}{3}$, respectively. The mass-independent length scale of the square-well potential leads to similar behavior for linear

and quadratic coupling, with α depressed below 0.5 for weak to moderate coupling and $\alpha = 0.5$ in the extreme strong coupling limit. For smaller values of the coupling, the deviation of the isotope effect exponent from 0.5 is generally in the same direction as that obtained in the strong coupling limit, with a larger deviation for weaker coupling.

We now consider the limit of arbitrarily deep double wells. In this situation, one would expect the problem to decouple into two uncoupled potential wells, with the particle occupying one well or the other. The ground state and first excited state will become degenerate, as will all subsequent pairs of excited states. At first sight, Eq. (2) seems to imply that λ will diverge, since the energy denominator goes to zero. However, for such low first excitation energies, one must consider the finite temperature generalization of Eq. (2),²⁶

$$\lambda = N(0) \sum_{kk'}^{(FS)} \sum_{n>n'} \sum_{n'} \frac{| \langle n | \langle k' | [(\nabla V \cdot \delta \mathbf{R})_{R_0} + \nabla_i \nabla_j V \delta \mathbf{R}_i \delta \mathbf{R}_j] | k \rangle | n' \rangle |^2}{E_n - E_{n'}} (f_{n'} - f_n), \quad (11)$$

where f_n is the thermal weighing factor $\frac{e^{-\beta E_n}}{\sum_i e^{-\beta E_i}}$. For $T \gg (E_1 - E_0)$, the difference between thermal factors for the ground state and first excited state goes to zero faster than the energy level difference, so that the contribution to λ from the nearly degenerate pair of lowest levels actually goes to zero in the limit of an infinitely deep double well. The sum over the other transitions in Eq. (16) yields the same result as that calculated for contributions from two decoupled potentials, with no reference to double-well character.

IV. APPLICATION TO HIGH- T_c MATERIALS

Several experimental and theoretical results suggest that strongly anharmonic potentials are relevant to the high- T_c oxides. X-ray absorption fine structure (EXAFS) experiments can be explained with a double-well potential of width 0.13 Å for *c*-axis motions of the apical oxygens in Y-Ba-Cu-O,¹⁸ although there are other plausible interpretations in terms of local structural distortions.²⁷ Although infrared measurements indicate that the mode in question has a frequency well above that derived from a local-mode solution to the proposed double-well potential, the infrared measurements probe $Q = 0$, whereas the EXAFS experiment probes the local lattice dynamics. Ion channeling experiments also indicate strong anharmonicity for vibrations involving the apical oxygens and the copper atoms.¹⁷ Frozen-phonon calculations yield multiple-well potentials for octahedral tilt motions in $\text{La}_{2-x}\text{M}_x\text{CuO}_2$ (Ref. 28) and for buckling motions in the oxygen chains of $\text{YBa}_2\text{Cu}_3\text{O}_7$.²⁹ X-ray scattering data suggest such a buckling distortion in the chains.³⁰ In addition, frozen-phonon calculations yield a strongly anharmonic, but not multiple-well, potential for the zone-center oxygen E_u mode in $\text{La}_{2-x}\text{Sr}_x\text{CuO}_2$.³¹ However, none of these multiple-well potentials represent generic

modes of the high- T_c oxides. The octahedral tilt is unique to materials with a single Cu-O plane. The chain buckling is unique to Y-Ba-Cu-O. There are several reasons why the apical oxygen vibrations are unlikely to be the sole contributor to a potential anharmonic mechanism. They are not present in several high- T_c materials, such as the "parent compound" electron-doped superconductor $\text{Sr}_{1-x}\text{Nd}_x\text{CuO}_2$ with $T_c = 40$ K.³² A model based entirely on these modes would seem to have difficulty accounting for the increase in T_c with an increasing number of Cu-O planes in the thallium and bismuth compounds, since the number of apical oxygens remains fixed as Cu-O planes are added. In any case, within our formalism, the potential suggested by the EXAFS experiments can produce a T_c of roughly 30 or 40 K for $\alpha \approx 0.0$, suggesting a significant, but perhaps not dominant, role for the apical oxygen modes. The most generic modes of possible multiple-well character would involve oxygen atoms in the Cu-O sheets, either buckling perpendicular to the sheets (similar to the in-plane behavior of the octahedral tilt mode), buckling parallel to the sheets (modes which are experimentally inaccessible due to screening), or vibrations along the bond (which could have double-well character at high Q due to Peierls-like distortions).

Before considering multiple-well potentials in detail, we note that the eigenvectors of harmonic normal modes will not be normal modes of the anharmonic system. These vibrations should in general couple to other modes, although it is possible that certain vibrations could act as effectively independent oscillators, as seen in certain metal hydrides.^{33,34} Consequently, the standard normal mode masses for these vibrations will not necessarily be physically relevant. Noting these difficulties, interpretation of frozen-phonon calculations for particular atomic displacements should proceed with caution, especially for complicated atomic distortions, such as the orthorhombic tilt mode. In the particular case of the orthorhombic

tilt, the strong dependence of the structural transition temperatures on ionic size^{36,37} implies that the anharmonic potential is strongly doping dependent, even for ions of the same valence. The frozen-phonon calculation for La_2CuO_4 (Ref. 28) should be treated as a representative example of the form of potential for this mode, not a definitive conclusion.

In a previous publication¹¹ we describe the application of an evolving quadrupolar potential to the variations of T_c and the isotope effect with varying Sr concentration in $\text{La}_{2-x}\text{Sr}_x\text{CuO}_4$.^{35,36} At low doping, the potential is taken to be roughly harmonic. As the doping increases, it is assumed that the outer relative minima form and steadily increase in depth until a multiple-well potential is obtained. In deference to the peculiarities of anharmonic lattices, we will discuss the behavior of several nonquadrupolar multiple-well potentials with analogous behavior under doping. Similar behavior for a wide class of potentials would lend some support to the physical relevance of this simplified model of anharmonicity. We do not propose that any particular potential is relevant to $\text{La}_{2-x}\text{Sr}_x\text{CuO}_4$; we merely wish to exhibit a general feature of multiple-well potentials.

We have examined one-dimensional double and triple wells. We also examined a triple well in the y direction coupled to a harmonic well in the x direction,

$$V(x, y) = ax^2 + (by^2 + cy^4 + dy^6) \frac{1}{fx^2 + 1} + gy^2 \frac{fx^2}{fx^2 + 1}. \quad (12)$$

We have also computed the variations in T_c and α for a two-dimensional triple-well potential of the form

$$V(r^2) = ar^2 + br^4 + cr^6 \quad (13)$$

with

$$r^2 = x^2 + y^2. \quad (14)$$

Finally, we have examined the behavior of an octopolar potential of similar dimensions.

Since a tight binding model suggests that the linear term in the electron-phonon coupling is absent for the orthorhombic tilt mode at the relevant phonon wave vector, these potentials have been examined for both linear and quadratic coupling. In the linear case, the distances between the outer minima of the potentials were taken in the range 0.22–0.25 Å. Quadratic coupling encompasses primarily the transition from the ground state of the local oscillator to the second excited state. The dominance of higher energy transitions implies that a quadratically coupled potential will be wider than a linearly coupled potential that yields the same frequency scale for the electron-phonon coupling. For this reason, the well widths for quadratically coupled potentials are in the range 0.4–0.5 Å. For each potential the oscillator mass has been taken as the mass of an oxygen atom. A larger oscillator mass would require a narrower potential.

For each of these potentials we obtain α near 0.5 at low doping, with a maximum substantially above 0.5 at intermediate doping (near the maximum T_c), and a rel-

atively constant value around 0.1 for high doping. The transition temperature peaks at ~ 30 K for intermediate doping. In the linear case, the electron-phonon coupling λ increases from ~ 1.0 for low doping, to ~ 2.0 for the highest doping.³⁸ The variation in λ is much less pronounced for quadratic coupling, with $\lambda \sim 2$ for all doping concentrations. For a more detailed account of the behavior of a particular evolving anharmonic mode, we refer to a previous publication.¹¹ The similar behavior of a broad class of potentials mitigates somewhat against the concerns stemming from the inadequacies of a harmonic normal mode description.

We now examine in detail a particular pair of quadratically coupled octopolar potentials which are designed to more closely mimic the structural instabilities which arise upon doping. The potentials are displayed in Figs. 2 and 3, which show the potential energy for tilts of the semirigid Cu-O octohedra. The magnitude of the tilt is expressed in terms of the displacement of the apical oxygen. Tilts toward the corners of the plot correspond to distortions to the low-temperature tetragonal (LTT) phase, while tilts to the sides correspond to the low-temperature orthorhombic (LTO) phase. In this case, the oscillator mass is set to 2.6 times the mass of an oxygen atom, the normal mode mass for the displacement in question. The potential of Fig. 2 is designed to mimic situation at doping levels of $x \sim 0.12$ near the incipient transition to the low-temperature tetragonal phase. The wells in the LTO directions have a minimum at 150 K, compared to a value of -75 K for the LTT wells. The deeper wells in the LTT directions are consistent with the low-temperature stability of the LTT phase at this doping level. The central well is set at zero energy. In the second potential the outer wells have flattened out, corresponding to the increased stability of the high-temperature tetragonal phase at higher doping levels. Assuming purely quadratic electron-phonon coupling, the first potential yields $T_c = 35$ K and $\alpha = 0.8$ for a fitted value of $\lambda = 2.0$. The second potential yields $T_c = 26$ K and $\alpha = 0.07$ for the same value of λ . In both cases the Coulomb repulsion is set at $\mu^* = 0.13$. The results are similar for μ^* in the range 0.05–0.30. Without

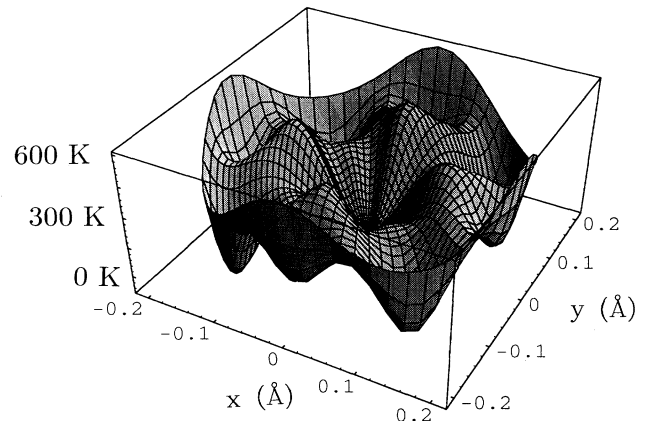


FIG. 2. Model octopolar potential for octahedral tilts in $\text{La}_{1.88}\text{Sr}_{0.12}\text{CuO}_4$.

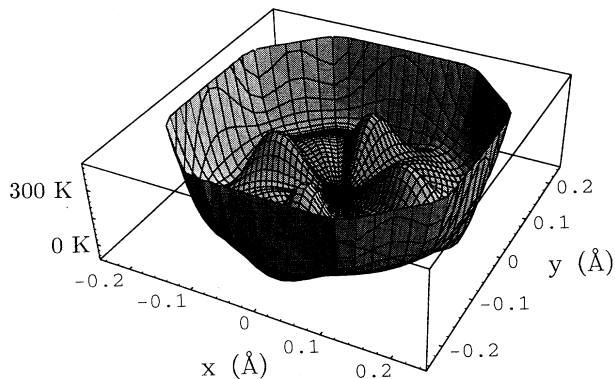


FIG. 3. Model octopolar potential for octahedral tilts in $\text{La}_{2-x}\text{Sr}_x\text{CuO}_4$ near the LTO \rightarrow HTT transition.

detailed experimental information on the form of the tilt mode potential, the present calculations must be considered as plausibility arguments. However, the theoretical results are fairly robust to variations in the detailed form of these potentials. The important qualitative features are the comparable magnitudes of the central and outer wells for the first potential and the flatness of the second potential.

Oxygen bucklings in the single Cu-O plane compounds may be dominated by semirigid tilt modes of the Cu-O octahedra, a fairly low-frequency motion. The multiple-plane compounds such as Y-Ba-Cu-O and Bi-Sr-Ca-Cu-O do not possess such a tilt mode. The relevant oxygen bucklings should therefore have a higher frequency, since the Cu-O skeleton must be nonrigidly distorted. The bucklings could be associated with narrow multiple-well potentials, as could vibrations along the Cu-O bond which are anomalously softened by a Peierls-like distortion. Several forms of multiple-well potentials can produce a near vanishing α for T_c on the order of 90 K. A quadrupolar potential of the form

$$V(r, \theta) = ar^2 + cr^6 + br^4 \cos 2\theta \quad (15)$$

with a distance of 0.14 Å between the origin and the outer minima can produce a T_c of 100 K with $\lambda = 1.3$ and $\alpha = 0.0$. A one-dimensional double well of the form

$$V(x) = ax^2 + bx^4 \quad (16)$$

with a distance of 0.12 Å between outer minima of depth 900 K produces a T_c of ~ 100 K with $\lambda = 2$ and $\alpha \sim 0$. A two-dimensional triple-well potential of the form of Eq. (13) can produce a T_c of roughly 80 K with $\lambda=2.0$ and $\alpha = 0.09$ for a distance of 0.10 Å between the outer minima. These examples assume linear electron-phonon coupling. A quadratically coupled double-well potential with a distance of 0.25 Å between the minima can also account for a high T_c and small α .

For each of these potentials the ionic mass has been set equal to the mass of an oxygen atom. The Coulomb pseudopotential μ^* has been fixed at 0.1; the results are relatively insensitive to this parameter. Quartic and sixth-order potentials also depress the isotope effect exponent. For example, a purely sixth-order linearly coupled one-

dimensional potential of the form $V(x) = 3.0 \times 10^8 x^6$ meV for x measured in Å produces a T_c of 93 K for $\alpha=0.01$.

Unfortunately, these narrow, high-frequency potentials do not generally have large values for the ionic part of λ , since the dipole matrix elements are not very large. Within our simple model, a large electron-phonon coupling for these potentials would have its origin in the electronic prefactor. Possible sources of a large electron-phonon coupling are local field effects,³⁹ ionic properties,⁴⁰ or Peierls-type distortions.⁴¹

If the hypothetical multiple-well potentials corresponded to the c axis polarized IR active modes, then one would expect an anomalously strong isotope effect in the frequencies of these modes under $^{16}\text{O} \rightarrow ^{18}\text{O}$ substitution. The lack of such an effect would imply that a plausible anharmonic potential must either correspond to a high- Q mode or an in-plane displacement which is not experimentally accessible due to screening.

We now examine the possibility that the higher transition temperatures of the multiple-plane compounds arise from interplanar coupling of oxygen buckling motions. We will assume a double-well potential for independent oxygen motions perpendicular to the plane with Hooke's law coupling between oxygen atoms in adjacent planes. The Hamiltonian is

$$H = \frac{p_1^2}{2m} + \frac{p_2^2}{2m} + a(q_1^2 + q_2^2) + b\left(\frac{1}{2}q_1^4 + 3q_1^2q_2^2 + \frac{1}{2}q_2^4\right) + 2cq_2^2, \quad (17)$$

where we have decomposed the motion into the harmonic normal mode coordinates. The coordinate q_1 describes oxygen atoms moving vertically in unison, while q_2 measures the amplitude of anticorrelated motion. Note that we are ignoring intraplanar dispersion. As the coupling constant c is increased, the degenerate ground state splits. The lower-frequency mode involves the atoms moving roughly in unison, such that the interplanar coupling is less important, whereas the higher-frequency mode becomes dominated by the interplanar spring. Although the average frequency of these two modes increases as the coupling becomes stronger, the lower-frequency mode dominates the superconductivity, limiting the increase in T_c to a few degrees. In addition, the decreased anharmonicity of the higher-frequency mode is inconsistent with the smaller isotope effect of the high- T_c compounds. In sum, within an anharmonic model, the higher T_c 's of the multiple-layer compounds is not due to interplanar coupling of c -axis modes. The source could instead reside in the larger number of buckling modes present in a multilayer system.

V. ISOTOPE EFFECT UNDER Cu-SITE SUBSTITUTION

Substitution of Zn, Fe, or Ni for Cu in $\text{YBa}_2\text{Cu}_3\text{O}_7$ and $\text{YBa}_2\text{Cu}_4\text{O}_8$ can have a dramatic effect on the isotope effect.¹³ Figure 4 reproduces experimental results for T_c versus α for various concentrations of these dopants. The substantial difference between the effects of the different

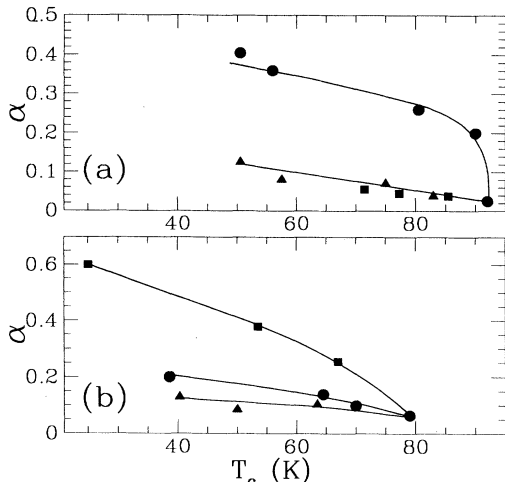


FIG. 4. Experimental results (Ref. 13) for the variation of α versus T_c for substitution of $M=\text{Fe}$ (circles), Ni (squares), and Zn (triangles) for Cu in (a) $\text{YBa}_2\text{Cu}_{3-x}\text{M}_x\text{O}_{7-\delta}$ and (b) $\text{YBa}_2\text{Cu}_{4-x}\text{M}_x\text{O}_8$. Curves are intended as a guide for the eye only.

dopants in the two compounds could be ascribed to different substitutional sites for the dopant atoms, although we do not examine this issue in detail here. Instead, we present a simple generic model of evolving anharmonicity which is consistent with the data. In particular, let us assume that the addition of dopant atoms destroys the delicate structural balance in the Cu-O planes necessary to produce anharmonic modes. Although one might expect the effect of the dopants to be rather inhomogeneous, we will model it by an evolving effective anharmonic potential as shown in Fig. 5. The variation in the potential is similar to that examined in our model of $\text{La}_{2-x}\text{Sr}_x\text{CuO}_4$. However, in this case the central well disappears more quickly so that the potential never produces $\alpha > 0.5$. We model the effect of different dopants by assuming that each dopant produces the same series

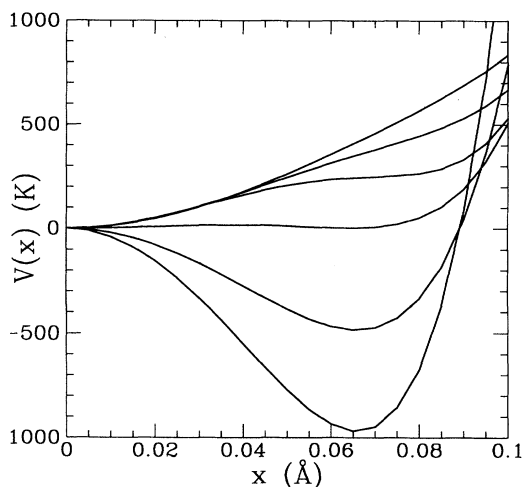


FIG. 5. Series of effective anharmonic potentials used to model Cu -site substitution in $\text{YBa}_2\text{Cu}_{3-x}\text{M}_x\text{O}_{7-\delta}$ and $\text{YBa}_2\text{Cu}_{4-x}\text{M}_x\text{O}_8$. The potentials become less anharmonic as the doping level increases.

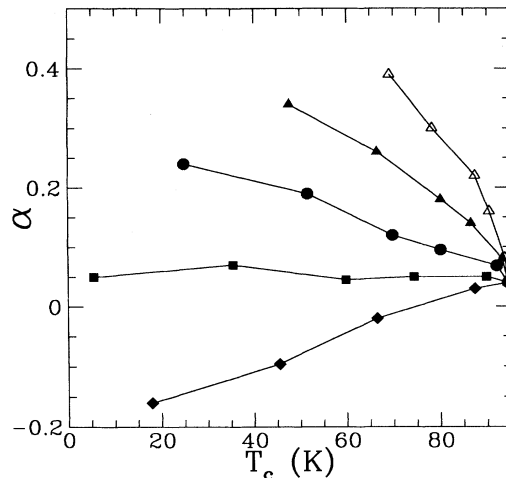


FIG. 6. Results for α vs T_c for the potentials of Fig. 2. Five different effects of doping on the electron-phonon coupling were considered, as discussed in the text: dopant A (open triangles), dopant B (filled triangles), dopant C (filled circles), dopant D (filled squares), and dopant E (filled diamonds).

of potentials, but with varying values of λ . We assume $\lambda = 2.0$ for the undoped material. Referring to Fig. 6, we have produced five theoretical curves. For dopant A, λ decreases from 2.0 to 1.20 at the lowest T_c value. For dopants B, C, D and E, the final values of λ are 0.95, 0.70, 0.45, and 0.20, respectively. In each case, the intermediate values of λ are obtained from a linear interpolation. The swift suppression of λ for dopant E produces an isotope effect that actually decreases with doping. The results for the variation in α with T_c span the breadth of the experimental behavior, with a similar functional form. However, considering the rather *ad hoc* nature of the proposed potentials, this result should be treated as simply a plausibility argument for the relevance of anharmonicity to the variations in T_c and α with Cu -site doping the the high- T_c oxides. In particular, this model provides a mechanism alternative to magnetic pair breaking from the addition of transition metal dopants.

VI. ISOTOPE EFFECT IN $\text{Y}_{1-x}\text{Pr}_x\text{Ba}_2\text{Cu}_3\text{O}_7$

In general, the substitution of other rare earths for Y in $\text{YBa}_2\text{Cu}_3\text{O}_7$ has little effect on the superconducting properties.⁴²⁻⁴⁵ However, introduction of Pr dramatically lowers the T_c , with superconductivity disappearing for Pr concentrations above 50%.⁴⁶⁻⁴⁸ Several models have been proposed to explain this behavior. If the Pr ions are tetravalent, they would reduce the carrier concentration, thereby suppressing superconductivity. On the other hand, since the $4f$ electrons of Pr are more extended than those of other magnetic rare earths, they may hybridize more readily, producing magnetic pair breaking. The experimental situation is somewhat unclear, with various results suggesting pair breaking,⁴⁹⁻⁵² valency,^{51,53} or carrier localization.⁵⁴ As the Pr concentration is increased, T_c decreases and the isotope effect exponent increases monotonically, reaching 0.5 for a Pr

concentration of 50% and a T_c of 30 K.¹² We have examined the implications of the pair breaking and valence models for reduction of T_c from the viewpoint of both an anharmonic model of high T_c and a nonspecific electronic model.

For illustrative purposes, we model pair breaking in the simplest possible manner. In the limit of a weak concentration of magnetic ions, the superconducting transition temperature is reduced by a mass-independent factor:⁵⁶

$$T_c = T_c^0 - A. \quad (18)$$

If we extrapolate this simple form to higher concentrations of magnetic ions, we obtain a simple qualitative formula for the isotope effect exponent as a function of T_c :

$$\alpha = \alpha_0 \left(\frac{T_c^0}{T_c} \right). \quad (19)$$

The increase in α upon doping is critically dependent upon the “base line” isotope effect α_0 present at maximum T_c . A much more thorough treatment of pair breaking yields qualitatively similar behavior, with a more pronounced variation in α with decreasing T_c and a similar sensitivity to the value of α_0 .⁵⁷ Within this treatment, large values of α_0 (roughly $\alpha_0 \sim 0.08$) are necessary to fit the experimental results for T_c versus α , at variance with the best characterized experimental results, which yield $\alpha = 0.02$.²⁴ However, the substantial scatter in α at maximum T_c evidenced in Fig. 7 precludes a definitive conclusion on the relevance of magnetic pair breaking.

Turning to the valence mechanism, we examine an electronic model, with a mass-independent electronic mode at 120 K and a harmonic phonon contribution at 480 K. A fit of a higher-frequency electronic mode to the exper-

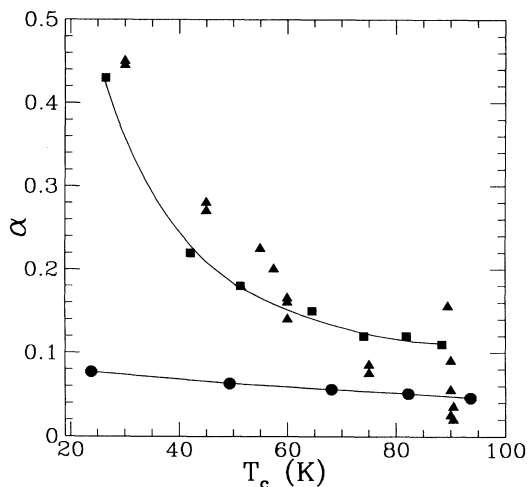


FIG. 7. The relationship between α and T_c in $Y_{1-x}Pr_xBa_2CuO_7$ for a valence model of T_c suppression. Experimental data (Ref. 12) (triangles) is compared with two electronic models, both with a 120 K mass-independent electronic mode and a 480 K harmonic phonon mode. One model (circles) has $\alpha(93\text{ K})=0.04$ and $\mu^* = 0.10$, the other (squares) has $\alpha(93\text{ K})=0.10$ and $\mu^* = 0.14$. In both cases, the doping selectively depresses the coupling to the electronic mechanism. Curves are intended as a guide for the eye.

imental values of T_c and α would produce a value of the electron-phonon coupling which is at variance with experimental results.⁵⁵ Within the valence model, we assume that the decrease in T_c is caused by a decrease in λ , which must be apportioned between the electronic and phonon-mediated terms in $\alpha^2 F$. If we assume that both terms are reduced by the same multiplicative factor, then the electronic mode will dominate for all values of T_c , keeping α small until superconductivity disappears. However, if the addition of Pr selectively depresses the electronic mechanism, while leaving the phononic mechanism undisturbed, then α will increase somewhat as Pr is incorporated. Results for the valence model are presented in Fig. 7. The increase in α is generally insufficient to explain the experimental results unless the phononic contribution to the coupling is large enough so that the isotope effect exponent at maximum T_c is roughly 0.10, substantially greater than the experimental value of 0.02.²⁴ A study of models with higher-frequency electronic modes yields similar results.

Treatments assuming magnetic pair breaking or selective suppression of a predominately electronic model yield too weak an increase in α with decreasing T_c if the “base line” isotope effect at maximum T_c is taken to be $\alpha = 0.02$. Since the detailed behavior of an anharmonic phonon model under Pr doping is unclear, we do not present a particular microscopic model. However, the previous discussion of Zn, Ni, and Fe doping indicates that strong variations in α are possible, even for a material with a vanishing isotope effect at maximum T_c .

The previous treatments have assumed that the density of states near the Fermi level is roughly constant. We note that a Van Hove singularity model for high- T_c superconductivity⁵⁸ appears consistent with the dependence of T_c on α . A thorough treatment of this situation is given by Carbotte *et al.*^{59,60} The effects of the valence model can be interpreted as a shift in the Fermi level away from the Van Hove singularity. As the singularity begins to leave the region $\pm\Omega_{\text{Debye}}$ from the Fermi level, the isotope exponent increases, since a small change in Ω_{Debye} will produce a large change in the total number of states within Ω_{Debye} of the Fermi level. Meanwhile, T_c will decrease since the singularity is leaving the region in which electron-phonon coupling is operative. If the peak of the singularity crosses the Ω_{Debye} threshold, one would expect α to peak, and then decrease. Perhaps a careful examination of α for the lowest values of T_c will reveal such a decrease in α . However, the Van Hove singularity model has several serious shortcomings as an explanation of high-temperature superconductivity.⁶¹

In sum, if the suppression of T_c in $Y_{1-x}Pr_xBa_2CuO_7$ is due to valence effects, then an anharmonic model with doping-dependent anharmonicity could reproduce the experimental data on the isotope effect. Under the same assumption, an electronic mechanism with a small phonon contribution is inconsistent with the small value of the isotope effect at maximum T_c . A mechanism based on magnetic pair breaking appears to fall victim to the small isotope effect at maximum T_c , although there is a certain amount of experimental scatter in the base-line value of α .

VII. POSSIBILITY OF $\alpha < 0$

In most theories of high-temperature superconductivity, a mass-independent mechanism is responsible for the large transition temperature. The small positive values of α are due to a small phonon contribution to T_c . Within a harmonic weak coupled BCS model, a negative value of α would be possible for a large value of μ^* , as revealed by a simple two-square-well model of superconductivity:

$$\alpha = \frac{1}{2} \left[1 - \left(\frac{\mu^*}{\lambda^* - \mu^*} \right)^2 \right]. \quad (20)$$

However, substantial negative values of α are unlikely, since weakly coupled phonons under the influence of a large μ^* will make a small contribution to T_c . This result also applies to a primarily electronic model of high T_c with a small phonon-derived isotope effect. In contrast, the anharmonic phonon model could produce significant negative α . For example, a decrease in λ will depress the isotope effect for a multiple-well anharmonic model. However, if the decrease in λ is accompanied by a reduction in the anharmonicity, then the effect on α is unclear. For example, the substitution of Ba or Sr for La in La_2CuO_4 changes the doping, therefore changing λ , but the same substitution also drives the system towards a structural phase transition, signaling a pronounced change in the anharmonicity of the phonons. Recent results on $\text{Bi}_{1.6}\text{Pb}_{0.4}\text{Sr}_2\text{Ca}_2\text{Cu}_3\text{O}_7$ with a T_c of 108 K have produced a very small negative isotope effect of -0.013 ± 0.002 ,¹³ which suggests the possibility of a larger negative isotope effect in the higher- T_c three-layer thallium compounds. In addition, recent site selective isotope effect experiments indicate an inverse isotope effect for substitution of planar oxygen atoms.⁶² The general trend of smaller α with a higher T_c suggests materials under high pressure as another candidate for $\alpha < 0$. Unfortunately, higher T_c 's imply stronger coupling. Referring to the strong coupling limit of an anharmonic α ,

$$\alpha = \frac{1}{2} - \frac{\lambda_M}{2\lambda}, \quad (21)$$

we note that competition between increasing λ and increasing λ_M may prevent α from attaining large negative values.

In any case, the measurement of a strong negative isotope effect in a particular high-temperature superconductor would lend support to an anharmonic model, which provides a natural explanation of such an effect. We note in passing that a large negative isotope effect need not be an unambiguous signal of anharmonicity. For example, $\alpha\text{-U}$ has a T_c of roughly 2 K and an isotope effect exponent of -2.2 .⁶³ Such a strong negative isotope effect in a strongly coupling superconductor cannot be explained by a large μ^* , but instead requires a novel mechanism. One could of course appeal to a similarly novel mechanism for the high-temperature superconductors. However, anharmonic effects, which can account for the anomalous values of α both above 0.5 and below 0.0, would provide the most natural explanation for a significant negative isotope effect in the high-temperature superconducting oxides.

VIII. CONCLUSIONS

Strongly anharmonic multiple-well phonons provide a means to explain several unusual properties of the high-temperature superconductors from within a BCS-like mechanism. An interesting experimental consequence of strong anharmonicity is a relatively strong mass dependence of the electron-phonon coupling. This dependence should be manifested in a mass dependence of the ratio $\frac{2\Delta}{kT_c}$. Under O^{18} substitution, λ would increase, so that this ratio should also increase. For plausible values of the anharmonicity, we estimate a 5–10% increase in $\frac{2\Delta}{kT_c}$ for complete $^{16}\text{O} \rightarrow ^{18}\text{O}$ substitution, if anharmonic effects are relevant for the high-temperature superconductivity.

ACKNOWLEDGMENTS

This research was supported by National Science Foundation Grant No. DMR88-18404 and by the Office of Energy Research, Office of Basic Energy Sciences, Materials Sciences Division of the U. S. Department of Energy under Contract No. DE-AC03-76SF00098. CRAY computer time was provided by the Office of Energy Research of the U.S. Department of Energy at the Pittsburgh supercomputing center. M.L.C. acknowledges support from the J. S. Guggenheim Foundation.

¹M. Shirai, N. Suzuki, and K. Motizuki, *J. Phys. Condens. Matter* **2**, 3553 (1990).

²Q. Huang, J. F. Zasadzinski, N. Tralshawala, K. E. Gray, D. G. Hinks, J. L. Peng, and R. L. Greene, *Nature* **347**, 369 (1990).

³J. M. Valles, Jr., R. C. Dynes, A. M. Cucolo, M. Gurvitch, L. F. Schneemeyer, J. P. Garno, and J. V. Waszczak, *Phys. Rev. B* **44**, 11986 (1991).

⁴H. A. Mook, M. Mostoller, J. A. Harvey, N. W. Hill, B. C. Chakoumakos, and B. C. Sales, *Phys. Rev. Lett.* **65**, 2712 (1990).

⁵Y. Koyama and H. Hoshiya, *Phys. Rev. B* **39**, 7336 (1989).

⁶P. B. Allen and Dierk Rainer, *Nature* **349**, 396 (1991).

⁷B. Sundqvist and B. M. Andersson, *Solid State Commun.*

76, 1019 (1990).

⁸M. Gurvitch and A. T. Fiory, *Phys. Rev. Lett.* **59**, 1337 (1987).

⁹V. H. Crespi and M. L. Cohen, *Solid State Commun.* **81**, 187 (1992).

¹⁰I. I. Mazin and O. V. Dolgov, *Phys. Rev. B* **45**, 2509 (1992).

¹¹V. H. Crespi and M. L. Cohen, *Phys. Rev. B* **44**, 4712 (1991).

¹²J. P. Frank, J. Jung, M. A.-K. Mohamed, S. Gyax, and G. I. Sproule, *Physica B* **169**, 697 (1991).

¹³H. J. Bornemann, D. E. Morris, H. B. Liu, A. P. B. Sinha, P. Narwankar, and M. Chandrchood (unpublished).

¹⁴W. E. Pickett, *Rev. Mod. Phys.* **61**, 499 (1989).

¹⁵S. J. L. Billinge, B. H. Toby, H. D. Rosenfeld, T. Sendyka,

- and T. Egami (unpublished).
- ¹⁶S. J. L. Billinge (private communication).
- ¹⁷R. P. Sharma, L. E. Rehn, P. M. Baldo, and J. Z. Liu, *Phys. Rev. Lett.* **62**, 2869 (1989).
- ¹⁸J. Mustre de Leon, S. D. Conradson, I. Batistić, and A. R. Bishop, *Phys. Rev. Lett.* **65**, 1675 (1990).
- ¹⁹J. C. K. Hui and P. B. Allen, *J. Phys. F* **4**, L42 (1974).
- ²⁰W. L. McMillan, *Phys. Rev.* **167**, 331 (1968).
- ²¹A. E. Karakozov and E. G. Maksimov, *Zh. Eksp. Teor. Fiz.* **74**, 681 (1978) [*Sov. Phys. JETP* **47**, 358 (1978)].
- ²²V. H. Crespi, M. L. Cohen, and D. R. Penn, *Phys. Rev. B* **43**, 12921 (1991).
- ²³V. Z. Kresin, *Bull. Am. Phys. Soc.* **32**, 796 (1987).
- ²⁴L. C. Bourne, A. Zettl, T. W. Barbee, III, and M. L. Cohen, *Phys. Rev. B* **36**, 3990 (1987).
- ²⁵P. B. Allen and R. C. Dynes, *Phys. Rev. B* **12**, 905 (1975).
- ²⁶J. R. Hardy and J. W. Flocken, *Phys. Rev. Lett.* **60**, 2191 (1988).
- ²⁷J. Jorgensen (private communication).
- ²⁸W. E. Pickett, R. E. Cohen, and H. Krakauer, *Phys. Rev. Lett.* **67**, 228 (1991).
- ²⁹R. E. Cohen, W. E. Pickett, and H. Krakauer, *Phys. Rev. Lett.* **64**, 2575 (1990).
- ³⁰W. Wong-Ng, F. W. Gayle, D. L. Kaiser, S. F. Wakins, and F. R. Fronczek, *Phys. Rev. B* **41**, 4220 (1990).
- ³¹R. E. Cohen, W. E. Pickett, H. Krakauer, and D. A. Papaconstantopoulos, *Phase Trans.* **22**, 167 (1990).
- ³²M. G. Smith, A. Manthiram, J. Zhou, J. B. Goodenough, and J. T. Market, *Nature* **351**, 549 (1991).
- ³³T. Springer, in *Hydrogen in Metals I*, edited by G. Alefeld and J. Völkl (Springer-Verlag, Berlin, 1978).
- ³⁴V. H. Crespi and M. L. Cohen, *Solid State Commun.* **83**, 427 (1992).
- ³⁵M. K. Crawford, W. E. Farneth, E. M. McCarron, III, R. L. Harlow, and A. H. Moudden, *Science* **250**, 1390 (1990).
- ³⁶M. K. Crawford, M. N. Kunchur, W. E. Farneth, E. M. McCarron, III, and S. J. Poon, *Phys. Rev. B* **41**, 282 (1990).
- ³⁷B. Büchner, M. Cramm, M. Braden, W. Braunisch, O. Hoffels, W. Schnelle, J. Harnischmacher, R. Borowski, A. Gruetz, B. Heymer, C. Hohn, R. Müller, O. Maldonado, A. Freimuth, W. Schlabitz, G. Heger, D. I. Khomskii, and D. Wohlleben, in *Proceedings of the NATO Advanced Study Institute, Physics and Material Science of HTSC II, Greece, 1991*, edited by R. Kossowsky (Kluwer, Dordrecht, in press).
- ³⁸S. Barišić, I. Batistić, and J. Friedel, *Europhys. Lett.* **3**, 1231 (1987).
- ³⁹C. Tarrío, E. L. Benitez, and S. E. Schnatterly, *Physica C* **193**, 34 (1992).
- ⁴⁰R. E. Cohen, W. E. Pickett, H. Krakauer, and D. A. Papaconstantopoulos, *Phase Trans.* **22**, 167 (1990).
- ⁴¹V. H. Crespi and M. L. Cohen (unpublished).
- ⁴²K. N. Yang, Y. Dalicaouch, J. M. Ferreria, B. W. Lee, J. J. Neumeir, M. S. Torikachvili, H. Zhou, M. B. Maple, and R. R. Hake, *Solid State Commun.* **63**, 515 (1987).
- ⁴³Z. Fisk, J. D. Thompson, E. Zirngiebl, J. L. Smith, and S. W. Cheong, *Solid State Commun.* **62**, 743 (1987).
- ⁴⁴P. H. Hor, R. L. Meng, Y. Q. Wang, L. Gao, Z. J. Huang, J. Bechtold, K. Forster, and C. W. Chu, *Phys. Rev. Lett.* **58**, 1891 (1987).
- ⁴⁵D. W. Murphy, S. Sunshine, R. B. Van Dover, R. J. Cava, B. Batlogg, S. M. Zahurak, and L. F. Schneemeyer, *Phys. Rev. Lett.* **58**, 1888 (1987).
- ⁴⁶L. Soderholm, K. Zhang, D. G. Hinks, M. A. Beno, J. D. Jorgenson, C. U. Segre, and I. K. Schuller, *Nature* **328**, 604 (1987).
- ⁴⁷Y. Dalicaouch, M. S. Torikachvili, E. A. Early, B. W. Lee, C. L. Seaman, K. N. Yang, H. Zou, and M. B. Maple, *Solid State Commun.* **65** 1001 (1987).
- ⁴⁸K. K. Liang, X. T. Xu, S. S. Xie, G. H. Rao, X. Y. Shao, and Z. G. Duan, *Z. Phys. B* **69**, 137 (1987).
- ⁴⁹J. L. Peng, P. Klavins, R. N. Shelton, H. B. Radousky, P. A. Hahn, and L. Bernardez, *Phys. Rev. B* **40**, 4517 (1989).
- ⁵⁰G. Y. Guo and W. M. Temmerman, *Phys. Rev. B* **41**, 6372 (1990).
- ⁵¹J. J. Neumeier, T. Bjornholm, M. B. Maple, and Ivan K. Schuller, *Phys. Rev. Lett.* **63**, 2516 (1989).
- ⁵²H. B. Radousky, *J. Mater. Res.* **7**, 1917 (1992).
- ⁵³Kyun Nahm, Bo Young Cha, and Chul Koo Kim, *Solid State Commun.* **72** 559 (1989).
- ⁵⁴J. Fink, N. Nücker, H. Romberg, M. Alexander, M. B. Maple, J. J. Neumeier, and J. W. Allen, *Phys. Rev. B* **42**, 4823 (1990).
- ⁵⁵T. W. Barbee, III, Marvin L. Cohen, and David R. Penn, *Phys. Rev. B* **44** 4473 (1991).
- ⁵⁶A. A. Abrikosov and L. P. Gor'kov, *Zh. Eksp. Teor. Fiz.* **39**, 1781 (1961) [*Sov. Phys. JETP* **12**, 1243 (1961)].
- ⁵⁷J. P. Carbotte, M. Greeson, and A. Perez-Gonzalez, *Phys. Rev. Lett.* **66**, 1789 (1991).
- ⁵⁸J. E. Hirsch and D. J. Scalapino, *Phys. Rev. Lett.* **56**, 2732 (1986).
- ⁵⁹E. Schachinger, M. G. Greeson, and J. P. Carbotte, *Phys. Rev. B* **42**, 406 (1990).
- ⁶⁰J. P. Carbotte and R. Akis, *Solid State Commun.* **82**, 613 (1992).
- ⁶¹D. R. Penn and M. L. Cohen, *Phys. Rev. B* **46**, 5466 (1992).
- ⁶²J. H. Nickel, D. E. Morris, and J. W. Ager, *Phys. Rev. Lett.* **70**, 81 (1993).
- ⁶³R. D. Fowler, J. D. G. Lindsay, R. W. White, H. H. Hill, and B. T. Matthias, *Phys. Rev. Lett.* **19**, 892 (1967).